Understanding diffraction patterns of disordered materials

The absence of translational periodicity and symmetry, and the rich structural complexity make it difficult to understand the order within disorder [1] in the structure of glassy, liquid, and amorphous materials. Indeed, as noted by Egelstaff in his review article in 1983 [2], determining the structure of disordered materials can be frustrating; although the underlying concepts have been known for a while, appropriate measurement methods for obtaining diffraction data of sufficient quality are usually not available. However, the advent of advanced instrumentation and measurement protocols makes it feasible to use quantum beam diffraction (X-ray diffraction (XRD) and neutron diffraction (ND)) techniques to reveal the structure of disordered materials at synchrotron and neutron facilities [3]. Moreover, a combination of diffraction measurement, advanced computer simulation, and topological analysis techniques enables us to understand the structure of disordered materials. In our work, attempts are being made to understand and characterize diffraction patterns from disordered materials measured at SPring-8 **BL04B2** and other quantum beam facilities with the aid of topological analyses based on atomic configurations obtained from reverse Monte Carlo (RMC) and/or molecular dynamics (MD) simulations, which reproduce experimental diffraction data.

The ND $S(Q)$ for glassy (g)-SiO_2, a canonical network-forming glass, exhibits a three-peak structure: Q_1 (first sharp diffraction peak (FSDP)), Q_2 (principal peak (PP)), and Q_3 (Fig. 1(a), bottom). Note that scattering vector Q is scaled by the nearest-neighbor atomic distance observed in real space to eliminate the effect of atomic size. Amorphous (a-)Si, possessing a fully tetrahedral network, has Q_2 and Q_3 (Fig. 1(a), middle), whereas only Q_3 is observed in the $S(Q)$ for g-$Cu_{50}Zr_{50}$ (Fig. 1(a), top), which has a typical dense random packing (DRP) structure. It is well known that the short-range structural unit of g-SiO_2 is a SiO_4 tetrahedron with a corner-sharing motif, giving rise to a large fraction of cavity volume (Fig. 1(b)) owing to the chemical contrast between silicon (fourfold) and oxygen (twofold) atoms. This structural feature is manifested by the appearance of a FSDP (periodicity: $2\pi/Q_{FSDP}$~4.2 Å, correlation length: $2\pi/\Delta Q_{FSDP}$~9.9 Å). Such a contrast is not found in a-Si, whose short-range structural unit is a $SiSi_4$ tetrahedron that results in the absence of FSDP. The average coordination number in g-$Cu_{50}Zr_{50}$ is approximately 12, which is much larger than those of others, suggesting that the PP is the signature of chemical bonds, because g-$Cu_{50}Zr_{50}$ has no chemical bond in its DRP structure.

To understand the origin of FSDP, we introduced a novel topological analysis based on modern mathematics: persistent homology together with the conventional ring size distribution analysis. The Si–O ring size distribution of g-SiO_2 glass is compared with those of crystalline polymorphs in Fig. 2. It is well known that silica glass (d = 2.21 g·cm^{-3}) exhibits a broad ring size distribution, although the sixfold ring is dominant (Fig. 2(d)). In contrast, α-cristobalite (d = 2.33 g·cm^{-3}) shows only sixfold rings (Fig. 2(a)). A large fraction of eightfold rings is observed in α-quartz (d = 2.65 g·cm^{-3}) (Fig. 2(b)), and coesite (d = 2.91 g·cm^{-3}) shows a variety of different ring sizes, similarly to g-SiO_2 (Fig. 2(c)). The Si-centric persistence diagrams (PDs) shown in Figs. 2(e-h) provide us with information on the shape of rings (how rings are buckled). The profile observed at b_k = 2.2 Å^2 in the Si-centric PD for α-cristobalite shows a large d_k of 7.4 Å^2, demonstrating that sixfold rings are symmetrical. However, d_k decreases with increasing density from α-quartz (Fig. 2(f)) to coesite (Fig. 2(g)), suggesting that the rings are significantly buckled in the high-density phases. The Si-centric PD for g-SiO_2 exhibits a characteristic vertical profile along with the death axis at b_k = 2.2 Å^2, which is in line with the formation of the FSDP in the glass. Indeed, our recent studies on densified g-SiO_2 confirmed this point [1]. Moreover, it is implied that this profile stretching from α-cristobalite to coesite is a signature of a good glass former; in other words, glass does not have a profile, which is similar to one specific crystalline phase.

Uncovering the difference between amorphous and liquid phases on the basis of diffraction and topology provides us with crucial information to understand the nature of glass formation. In this section, we compare g-/l-SiO_2 and a-/l-Si. As mentioned in the previous section, g-SiO_2 exhibits a FSDP (Q_1) not only in the ND $S(Q)$ (Fig. 3(a), bottom) but also in the XRD $S(Q)$ (Fig. 3(a), top). However, the PP (Q_2) is visible only in the ND $S(Q)$ (Fig. 3(a)), because it reflects the packing fraction of oxygen atoms [3,4], since neutrons are sensitive to O–O correlation, while X-rays are more sensitive to Si–Si

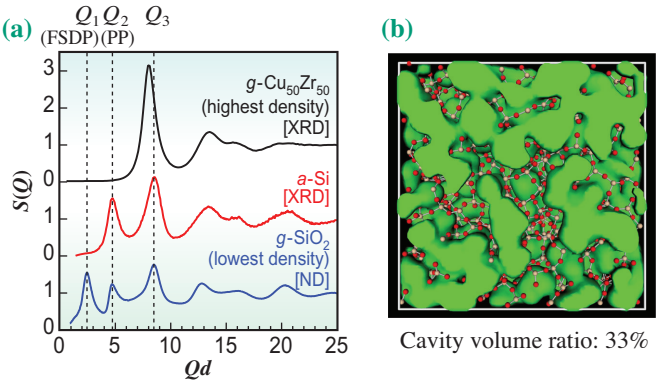

Fig. 1. Structure factors, $S(Q)$, for g-$Cu_{50}Zr_{50}$, a-Si, and g-SiO_2 [4] **(a)** and visualization of cavities (highlighted in green) in g-SiO_2 (b) [5].

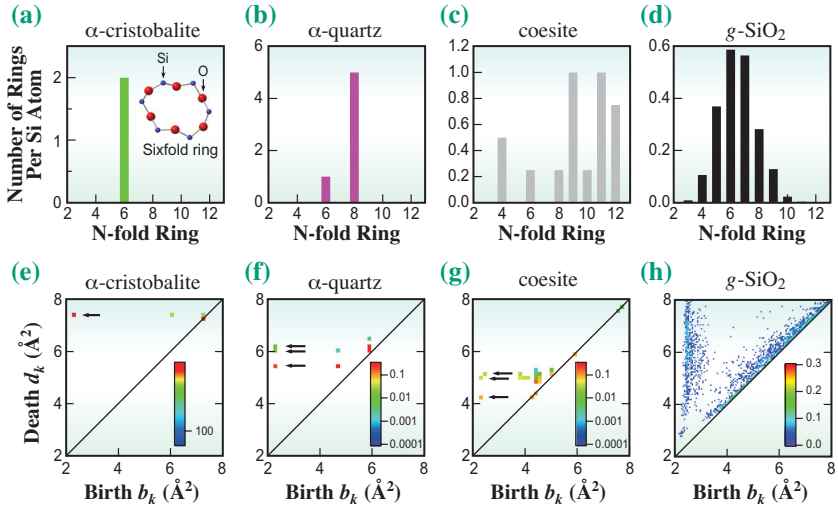

Fig. 2. Ring size distributions **(a–d)** and Si-centric PDs **(e–h)** of silica polymorphs [4].

correlations. The FSDP in the XRD $S(Q)$ is prominent in l-SiO_2, shown as a red curve in Fig. 3(a), suggesting that the Si–O covalent bond is strong even in liquid (2323 K) [4]. This behavior is consistent with the Si-centric PDs (Fig. 3(c)), in which the profile of the liquid phase is identical to that of the glassy phase, because density (glass: 2.21 g·cm^{-3}; liquid: 2.1 g·cm^{-3}) and Si–O coordination number differences (glass: 4.0; liquid: 3.9) are small between these two phases in SiO_2. On the other hand, both the XRD $S(Q)$ (Fig. 3(b)) and Si-centric PDs (Fig. 3(d)) for Si show significant differences between amorphous and liquid phases. The prominent Q_2 observed in the XRD $S(Q)$ of a-Si diminishes and overlaps with Q_3, suggesting that the density of the liquid phase is higher than that of the amorphous phase. This behavior is consistent with the Si-centric PDs for Si, because the characteristic vertical profile along with the death axis observed at $b_k \sim 1.5$ Å^2 in the amorphous phase is diminished in the liquid phase, suggesting that the liquid structure is highly densely packed. Indeed, density (amorphous: 2.3 g·cm^{-3}; liquid: 2.57 g·cm^{-3}) and Si–Si coordination number differences (amorphous: 4.0, liquid: 5.7) are large between the two phases in Si in comparison with SiO_2. This behavior is consistent with the fact that a-Si is a semiconductor and l-Si is a metal.

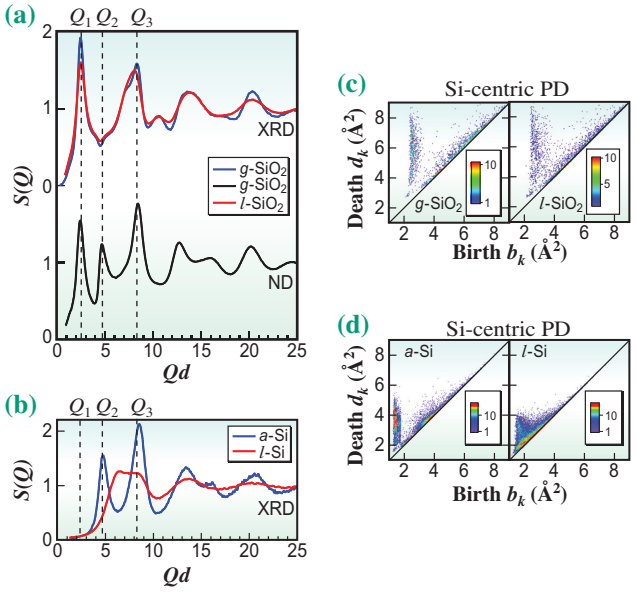

Fig. 3. Structure factors, $S(Q)$, for g- and l-SiO_2 (2323 K) **(a)**, and for a- and l-Si (1770 K) **(b)**, and Si-centric PDs for g- and l-SiO_2 **(c)**, and a- and l-Si **(d)**. [4]

In this article, we describe attempts to understand the origin of diffraction peaks from disordered materials with the aid of topological analyses based on structural models obtained by reverse Monte Carlo (RMC) modelling and/or molecular dynamics (MD) simulations. Combining quantum beam measurements and advanced simulations with topological analyses would be a very promising way to extract the hidden order in disordered materials. The results of advanced analysis will lead to the capability to forge a new path for designing novel functional disordered materials.

Shinji Kohara[a,*], Yohei Onodera[b,a] and Osami Sakata[a]

[a] Research Center for Advanced Measurement and Characterization, National Institute for Materials Science
[b] Institute for Integrated Radiation and Nuclear Science, Kyoto University

*Email: KOHARA.Shinji@nims.go.jp

References

[1] Y. Onodera *et al.*: NPG Asia Mater. **12** (2020) 85.
[2] P.A. Egelstaff: Adv. Chem. Phys. **53** (1983) 1.
[3] S. Kohara and P.S. Salmon: Adv. Phys. X **1** (2016) 640.
[4] *Y. Onodera, S. Kohara, S. Tahara, A. Masuno, H. Inoue, M. Shiga, A. Hiraha, K. Tsuchiya, Y. Hiraoka, I. Obayashi, K. Ohara, A. Mizuno and O. Sakata: J. Ceram. Soc. Jpn.* ***127*** *(2019) 853.*
[5] Y. Onodera *et al.*: NPG Asia Mater. **11** (2019) 75.